energy&fuels

Article

pubs.acs.org/EF

Fischer–Tropsch Synthesis Catalyzed by Solid Nanoparticles at the Water/Oil Interface in an Emulsion System

Dachuan Shi,[†] Jimmy A. Faria,[†] Ali A. Rownaghi,[‡] Raymond L. Huhnke,[‡] and Daniel E. Resasco*,[†]

[†]School of Chemical, Biological, and Materials Engineering, and Center for Interfacial Reaction Engineering (CIRE), University of Oklahoma, Norman, Oklahoma 73019, United States

[‡]Department of Biosystems and Agricultural Engineering, Oklahoma State University, Stillwater, Oklahoma 74078, United States

Supporting Information

ABSTRACT: Fischer–Tropsch synthesis (FTS) was carried out in a water/oil mixture medium, using a Ru catalyst supported on a multi-walled carbon nanotube/MgO–Al_2O_3 hybrid as a catalyst support. The nanohybrid particles at the water/oil interface facilitated and stabilized the formation of water-in-oil emulsion, giving rise to an oil/emulsion/water trilayer liquid structure. FTS occurred at the emulsion phase with much higher conversion rates than those in oil single-phase reactions, yielding products with Anderson–Schulz–Flory distribution. Alkane-enriched hydrocarbons migrate to the top oil phase, while short alcohols remain in the bottom water phase. Thus, this multiphase liquid structure facilitates the separation of products according to their solubility in different phases. This significant advantage of combined reaction and separation is unique to the multiphasic system. In addition, differences in solubility could be used to enhance tolerance against impurities and catalyst poisons in the syngas feedstock. As a preliminary case study, hydrochloric acid and pyridine were chosen as model contaminants commonly found in biosyngas. It was found that their presence did not affect the catalytic activity as severely as could be expected in a conventional FTS process. Thus, emulsion-phase FTS could be beneficial to operations where syngas production such as biomass gasification and FTS are integrated. The several advantages of using emulsion systems in FTS are discussed in light of the current results.

1. INTRODUCTION

Fischer–Tropsch synthesis (FTS) is a well-established technology for gas-to-liquid conversion in the production of predominately aliphatic straight-chain hydrocarbons. FTS is an important route for use of syngas (CO/H_2) generated from gasification of coal and biomass and steam reforming of natural gas and has been gaining ever-growing interests in recent decades because of increasing demands for sustainability and alternative sources to conventional oil. Commercial FTS is performed in three major reactor types: fluidized bed, fixed bed, and slurry bubble columns; the last two involve organic solvents as reaction media.[1] Multiphase reactors combining gas (syngas), liquid (reaction media and products), and solid (catalysts) are considered most promising.[2] For example, slurry bubble columns have the advantages of good heat transfer, high catalyst efficiency, convenience for catalyst regeneration/reloading, and lower costs.[3,4] Therefore, improvement in liquid-phase FTS has practical and industrial appeal.

Because of their high surface area, chemical inertness, and good mechanical strength, carbon nanomaterials have demonstrated to be excellent catalyst supports for FTS[5] as well as in other reactions.[6−10] For example, in a recent study, Galvis et al.[11] found that, when using carbon nanofibers as the support, Fe nanoparticles gave FTS conversions to low olefins over 50%, as compared to only 10% when γ-Al_2O_3 was used as the support. It was proposed that the much stronger interaction of γ-Al_2O_3 with the Fe nanoparticles impeded the formation of iron carbide, the catalytically active phase. In addition, carbon nanotubes (CNTs) have been proposed to increase catalyst activity, probably because of enhanced H_2 uptake and spillover.[12] Our group has recently reported a novel reaction system,[13] in which metal-doped CNT–inorganic oxide hybrids simultaneously stabilize emulsion because of their amphiphilic nature and catalyze reactions at the water/oil interface.

Here, we explored the application of the emulsion reaction system in FTS, in which both water and decalin are present as the reaction medium. A Ru catalyst supported on a multi-walled CNT/MgO–Al_2O_3 hybrid was used as a catalyst. Hydrocarbon and short alcohol products spontaneously partition in the decalin and water phases, respectively, fulfilling the initial objective of product separation. Much higher CO conversion rates were obtained in the emulsion system than in the decalin single phase. Also, significant differences in product distribution were observed, which may result in additional benefits to the use of emulsions for FTS. Finally, the potential benefit of the emulsion system to enhance tolerance to contaminants was explored by conducting the FTS reactions in the presence of hydrochloric acid and pyridine, which are common biosyngas impurities. The preliminary results demonstrate a higher impurity tolerance in the emulsion system, which might lead to interesting industrial applications.

2. EXPERIMENTAL SECTION

Ru/CNT hybrid catalysts were prepared via conventional incipient wetness impregnation. In this method, $RuCl_3$ (99.98%, hydrate, Sigma-Aldrich), used as the metal precursor, was dissolved in water and impregnated dropwise onto a determined amount of CNT hybrid (~70 wt % CNTs and balance of MgO–Al_2O_3 support,[14] kindly

Received: June 26, 2013
Revised: September 8, 2013
Published: September 9, 2013

   dx.doi.org/10.1021/ef401198m | Energy Fuels 2013, 27, 6118–6124

donated by Southwest Nanotechnologies, Inc.). The sample was then dried for approximately 12 h in a vacuum oven at 80 °C and subsequently annealed in flowing He at 400 °C for 3 h, followed by calcination at 200 °C in a conventional furnace for 2 h in air and later in He for 5 h. In an alternative method, the first He annealing step was replaced by reduction in a H_2/He (10% H_2) mixture flow. The characteristics of the two catalysts, denoted as catalysts 1 and 2, are summarized in Table 1. Their surface areas were determined by

Table 1. Characteristics of the Two Catalysts Investigated

catalyst	distinctive post-impregnation step	mean size (nm)	surface area (m^2/g)	Ru loading (%)
1	annealed in He	4	268.4	3.7
2	reduced in H_2/He	1.5	260.6	3.5

Brunauer–Emmett–Teller (BET, Micromeritics, ASAP 2000), and their Ru loadings were determined by inductively coupled plasma (ICP, Galbraith Laboratories), along with the mean particle sizes based on transmission electron microscopy (TEM, JEOL 2000-FX). The FTS reaction was performed in a 100 mL stainless-steel Parr autoclave batch reactor. In a typical experiment, 200 mg of catalyst, 15 mL of decalin (mixture of *cis* + *trans*, anhydrous, ≥99% purity, Sigma-Aldrich), and an equal volume of water (HPLC grade, Fischer Scientific), which emulsifies upon stirring, were added to the reactor vessel. The reactor was sealed, purged, and pressurized in H_2 to 400 psi for a reduction period of 12 h at 250 °C. After reduction, the reactor was cooled to room temperature and purged with fresh H_2 again. Finally, syngas was introduced at the desired H_2/CO ratio until a total pressure of 600 psi was reached. The actual composition of the gas was determined by thermal conductivity on a gas chromatography–thermal conductivity detector (GC–TCD, Carle 400 AGC). The reaction was conducted in the isolated batch mode at 200 °C for 12 h at a constant stirring rate of 700 rpm. Conversion was monitored as a function of time by the pressure change observed during the reaction. At the end of the reaction period, the gas-phase products were analyzed on the GC–TCD. The liquid-phase products were first filtered from which two immiscible layers of clear liquids were obtained. These phases were analyzed separately by gas chromatography–mass spectrometry (GC–MS, QP2010S, Shimadzu) and gas chromatography–flame ionization detector (GC–FID, Agilent 6890).

3. RESULTS AND DISCUSSION

3.1. Stabilization of Emulsions by Catalytic Nanohybrids. Figure 1a shows an optical microscopy image of the emulsion formed upon stirring the mixture mentioned in the Experimental Section. The microscopy image shows droplet sizes in the range of 1–10 μm. An optical image of the mixture is displayed in Figure 1b, in which the dark top part consists of water-in-oil emulsion,[15] with decalin as the continuous phase, while the clear bottom part is the free aqueous phase. In previous studies of our group, the emulsion was prepared by ultrasound sonication, which resulted in very stable emulsions that remained almost unaltered for more than 10 days.[13,15] Without ultrasound sonication, the emulsion can be sustained under constant stirring, but when left standing, the droplets collapse as denoted by the emergence and gradual enlargement of a clear top oil phase and gradual enlargement of the bottom water phase. This situation is desirable to easily break the emulsion, separate the products from the different phases, and recover the catalyst after reaction. It should be noted that, despite the elevated temperatures during the reduction and reaction steps, the small reactor volume used and the relatively large amount of water present in the system allowed for the vapor pressure of water to reach the saturation pressure with a relatively small fraction of water vaporization; therefore, the majority of the water present inside the vessel was in liquid form throughout the reaction (see the calculation in the Supporting Information).

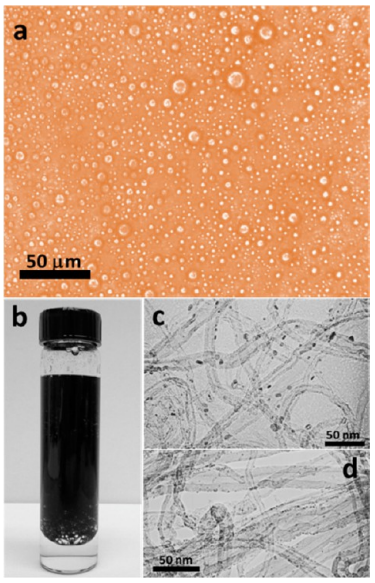

Figure 1. (a) Optical microscopy image of an emulsion formed by stirring a 1:1 mixture of decalin and water in the presence of the Ru/CNT nanohybrid. (b) Optical image of the emulsion system. TEM image of (c) catalyst 1 and (d) catalyst 2.

Panels c and d of Figure 1 show TEM images of the catalytic nanohybrids used in this study. Unless otherwise specified, catalyst 1 was used for most of the catalytic experiments described below. As shown in Figure 1c, Ru particles in this catalysts were in the 2–6 nm size range and uniformly deposited onto CNTs. Catalyst 2 (Figure 1d) had smaller and more uniform particles (1–2 nm range).

3.2. FTS in the Emulsion System. As illustrated in Figure 2a, when a low H_2/CO ratio of 1.2 (close to biosyngas composition[16,17]) was used, a complex variety of products, consisting of alkanes, alkenes, and long-chain alcohols, was obtained. After 6 h of reaction at 200 °C and 600 psi of initial pressure, with a catalyst mass to liquid of 5 mg/mL, the CO conversion was 38.1%. To simplify the analysis, a higher H_2/CO ratio of 3.5 was adopted along with 200 mg of catalyst and the FTS reaction period was extended to 12 h. The liquid products were found to be predominantly alkanes dissolved in the decalin phase (Figure 2b). A small amount of isopropanol, the only oxygenated product observed, was detected in the water phase. The total pressure decreased from 600 to 290 psi (both measured at room temperature, before and after reaction).

The hydrocarbon product distribution is summarized in panels a and c of Figure 3. It can be seen that the liquid hydrocarbons follow a trend that highly resembles the typical Anderson–Schulz–Flory (ASF) distribution.[18] Fitting this distribution with the ASF equation (Figure 3c) resulted in a chain growth probability of 84%, which is typical of Ru catalysts, as reported by Dry on fluidized- and fixed-bed reactors.[19] It should be noted that, at shorter reaction times (low conversions), products other than alkanes were also obtained (see Figure S3 of the Supporting Information). The presence of these products at low conversions, mainly alkenes, indicates that at least part of the alkane products observed at higher conversions are from secondary hydrogenation of

dx.doi.org/10.1021/ef401198m | *Energy Fuels* 2013, 27, 6118–6124

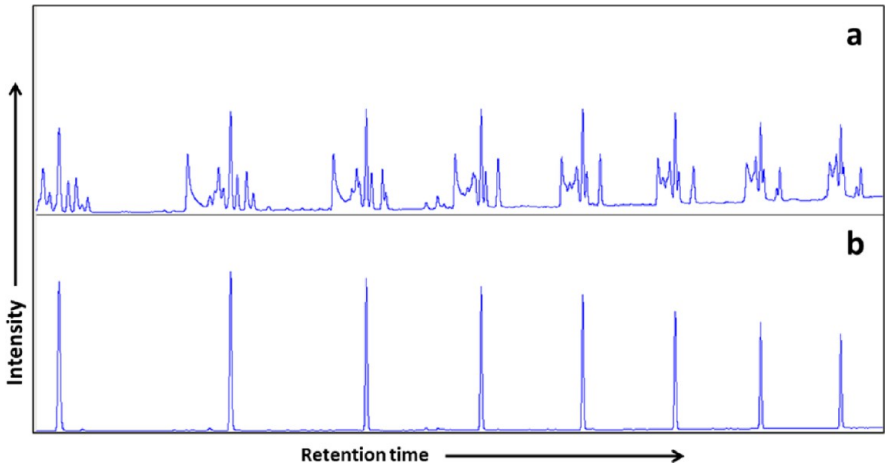

Figure 2. Representative sections of GC chromatographs for products in the decalin phase with (a) syngas ratio (H_2/CO) of 1.2, 6 h of reaction, and 150 mg of catalyst and (b) syngas ratio (H_2/CO) of 3.5, 12 h of reaction, and 200 mg of catalyst. Both reactions were at 200 °C.

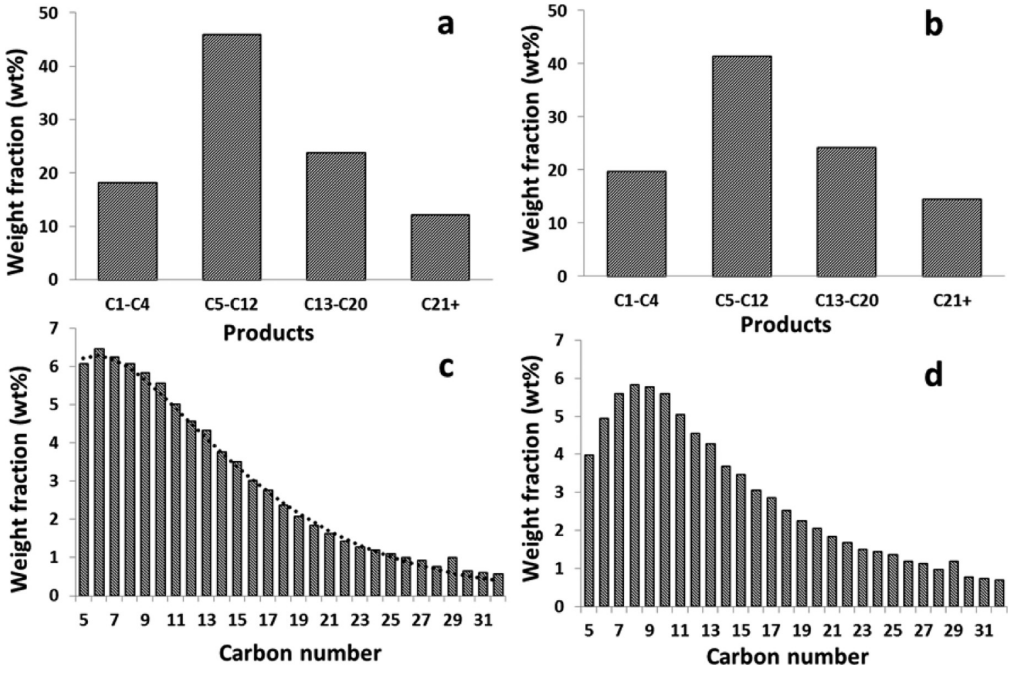

Figure 3. Weight distribution of hydrocarbon products obtained in the emulsion system over catalyst 1, larger Ru particles: (a) overall and (c) liquid phase, with the dotted line denoting fittings by the ASF distribution equation, and catalyst 2, smaller Ru particles: (b) overall and (d) liquid phase.

alkenes. Another reaction path that has been previously observed and leads to the secondary conversion of alkenes is the re-adsorption and re-insertion in the growing hydrocarbon chains.[20] However, this re-insertion would lead to variations from the ASF distribution, which are not observed in this case, which would indicate that the olefin/alkane ratio in this case is only determined by the extent of secondary hydrogenation of the olefin products.

At the end of the 12 h run, the CO conversion was determined to be 96%. Liquid hydrocarbons represent more than 80 wt % of the total hydrocarbon products. Gas products consisted of mainly methane and very small amounts of the C_2−C_4 fraction because of the relatively high H_2/CO ratio and reaction temperature, which might lead to increased surface mobility of the methane precursor.[21−23] Gas-phase analysis also indicated that only 3% of the initial CO was converted to CO_2 via the water-gas shift (WGS) reaction, despite the presence of excess water.

The initial CO conversion rate was determined to be 28.1 mol of CO (mol of Ru)$^{-1}$ h^{-1}, which corresponds to a turnover frequency (TOF) of 0.0282 s^{-1}, assuming a Ru dispersion based on TEM observations of 0.33. These values are in the upper range among those reported for Ru catalysts.[24−26] Catalyst 2, with much smaller and uniform particles (1−2 nm), had a much higher activity of 73.9 mol of CO (mol of Ru)$^{-1}$ h^{-1} but with a corresponding initial TOF of 0.0149 s^{-1}.

The higher TOF observed on larger Ru particles agrees well with previous studies on both Ru[27] and CO[28] catalysts, in which the higher TOF for larger particles was ascribed to the presence of more active sites on planar terraces. Despite some difference in activity, the product distributions (overall and liquid products) were similar on both catalysts, as summarized in panels b and d of Figure 3.

dx.doi.org/10.1021/ef401198m | *Energy Fuels* 2013, 27, 6118−6124

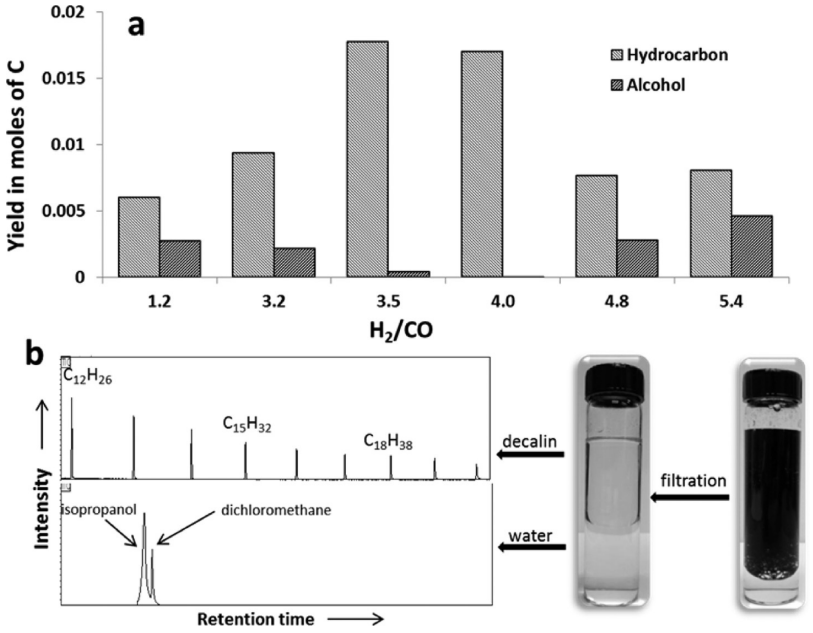

Figure 4. (a) Liquid-phase product yields at different H_2/CO ratios. (b) Representative sections of GC chromatographs for products in decalin and water phases.

The decalin single-phase reaction was conducted under otherwise exactly the same conditions (see the Supporting Information for whole-range chromatographs). In comparison to the results in the emulsion system, the CO conversion in the single-phase system was drastically lower, i.e., only 34.1% after 12 h, instead of 96%, with almost no hydrocarbon products larger than C_{10}. The results agree well with previous FTS studies, which report that adding small amounts of water vapor to syngas feed resulted in enhanced conversion rates and higher product selectivity toward longer chain hydrocarbons.[29−31] Various mechanisms to explain the important effect of water in the feed have been proposed in the literature, including water-assisted intraparticle transport of syngas and hydrocarbons[32] and water-shuttled transport of hydrogen to the active site, where hydrogen-assisted CO dissociation occurs.[33] In our case, in addition to the intrinsic promotion effects of adsorbed water, advantages unique to emulsions are expected to further contribute to the pronounced improvement over oil single-phase FTS. The formation of small droplets of water-in-oil dramatically increases catalyst dispersion and interfacial surface areas between the organic and aqueous phases. This enhancement results in improved contact between catalysts and reactants and much better mass transport between the two phases. As a result, produced molecules can be continuously removed from the reacting emulsion phase to other phases based on their differences in solubility (see the results below). In addition to facilitating the collection of the products, the spontaneous product migration may help to clean the catalyst surface more effectively, lowering the catalyst deactivation rate.

An important conceptual point must be raised here. It is well-known that the driving force that determines the chemical reaction and diffusion rates is given by thermodynamic properties, such as chemical affinity, chemical potential, or activity. Only in ideal reaction mixtures is it possible to express the reaction rates as a function of the concentration of the species present in the system.[34] Specifically, in the case of a reactant or a product with low solubility in one of the phases, this concept plays a very important role. Boudart et al.[35] noted that, when a component distributed in more than one phase reaches thermodynamic equilibrium, its chemical potential is the same in both phases. Therefore, the presence of a given species in one phase should equally affect the catalyst, regardless of the phase in which is present. However, the chemical potential of a given component may remain low in a phase with low solubility when the rate of mass transfer in that phase is so low that the phases are not in thermodynamic equilibrium. Therefore, the cleaning of a surface by migration to the other liquid phase implies that, under vigorous mixing, the product is transferred to the phase of higher solubility (e.g., alkanes in decalin) but the transport back to the catalyst surface in the phase of lower solubility is inhibited by mass-transport limitations.

The production of short alcohols was found to increase as the syngas composition deviated from the H_2/CO ratio of 4 (Figure 4a). These results can be used to illustrate the reaction/separation advantages of the emulsion system. Representative sections of GC chromatographs of decalin and water phases from the reaction with a syngas ratio of 5.4 are presented in Figure 4b. As shown, alcohol and hydrocarbon products were collected in the respective phases in which they were soluble, without any detectable crossover to the other phase. Longer alcohols partition more preferentially in the oil phase. Current commercial interest exists toward the $C_1−C_4$ alcohol range produced from FTS.[36] As shown here, in an emulsion system, they could be conveniently separated and collected in the aqueous phase, directly in the synthesis reactor. Besides alkanes, alkenes, and alcohols as target products, a variety of less desirable side products, such aldehydes, ketones, acids, esters, and carbon, is typically obtained in industrial FTS. These products are known to deactivate the catalysts and foul and/or etch the system. The oil/emulsion/water structure is an effective system to deal with this issue. Undesirable water-soluble products could migrate into the aqueous phase, leaving the reaction zone in the middle emulsion phase less affected and, thus, less severe catalyst deactivation.

dx.doi.org/10.1021/ef401198m | *Energy Fuels* 2013, 27, 6118−6124

The change in product composition or relative alcohol yield with the changing H_2/CO ratio is an interesting aspect to analyze further. The change can be rationalized by taking into account the general patterns of primary FTS products together with the role of the presence of a liquid water phase. Because isopropanol is the only alcohol observed in the water phase, it is reasonable to conclude that this alcohol is produced by hydration of propene[37,38] rather than that directly from oxygen termination of the FTS. The latter would result in a range of primary alcohols.[39] In contrast, hydration is known to occur preferentially on a secondary carbon.[40] On the low H_2/CO ratio range (i.e., below 4), the alkene yield was observed to decrease as the ratio increased.[41,42] This decrease in the alkene yield resulted in a concomitant decrease in the alcohol yield. In contrast, as discussed below, on the high H_2/CO ratio range (i.e., above 4), a further increase in the ratio led to higher CO conversions with an increased isopropanol yield. In this case, however, longer alkenes do not seem to undergo hydration. One may speculate that, once formed, they tend to migrate to the organic phase, where hydration might not occur as readily. At the other end, ethylene hydration to ethanol was not favored either, because it would involve a primary carbonium ion as an intermediate, which is much less stable than a secondary carbonium ion, as in the case of propylene hydration. While these speculations should be subject to further experimental examinations, the current observations imply that reaction in an emulsion system may provide unique possibilities for control of FTS selectivity.

The chain growth probability (α) values and CO conversion levels obtained at varying H_2/CO ratios are listed in Table 2.

Table 2. Conversions and Chain Growth Probability (α) Values in Some FTS Reactions in This Study

H_2/CO ratio	1.2[a]	3.2	3.5	4.0	4.8	5.4	3.5[b]
conversion (%)	38.1	58.5	96.0	96.1	93.4	90.9	87.8
α value (%)	N/A	80.0	84.3	84.2	81.2	81.2	86.6

[a]A 6 h reaction. [b]A 6 h reaction, with catalyst 2.

It is generally observed that the CO consumption rates increase with H_2 pressures. As described in previous studies, the rate increases with CO pressures only below a threshold value, beyond which the rate is zero-order with respect to CO pressure.[43−45] The variation in conversion levels observed here for different H_2/CO ratios reflect the combined effects of both pressures. In all cases, reactions started with much higher CO pressures than the threshold value for zero-order reaction (e.g., ∼50 psi[46]). Therefore, at the beginning of each run, only the H_2 pressure was rate-determining. Thus, lower conversions were obtained at relatively low H_2/CO ratios of 1.2 and 3.2.

Syngas often contains other components besides H_2 and CO. The inorganic impurities include HCl, H_2S, COS, NH_3, etc., which are catalyst poisons. Despite a multistep and integrated approach that is usually involved in syngas conditioning,[47] impurities are only eliminated down to a certain level because of economic considerations and technological limitations. With higher solubility in water and more restricted mass transfer in oil of these impurities and a confined location of the catalyst because of the hydrophobicity of the supporting CNTs, it is possible to further lower the impact of the trace amounts of poisons to catalyst activity in emulsion-phase FTS. Here, again, the interplay of chemical potential, thermodynamic equilibrium, and mass-transport effects must be considered when analyzing the effect of impurities in the emulsion system. As mentioned above, only in ideal reaction mixtures is it possible to express the reaction rates as a function of the concentration. Here, if a catalyst poison having low solubility in one of the phases is present in the system, its chemical potential is the same in both phases. Therefore, the presence of a catalyst poison in one phase should equally affect the catalyst, regardless of the phase in which this is present. However, if because of the low solubility, the transport into the phase that contains the catalyst is slow, the chemical potential of the poison will remain low, because the phases are not in thermodynamic equilibrium.

To test this concept, we performed FTS in the emulsion system in the presence of HCl in one case and pyridine in

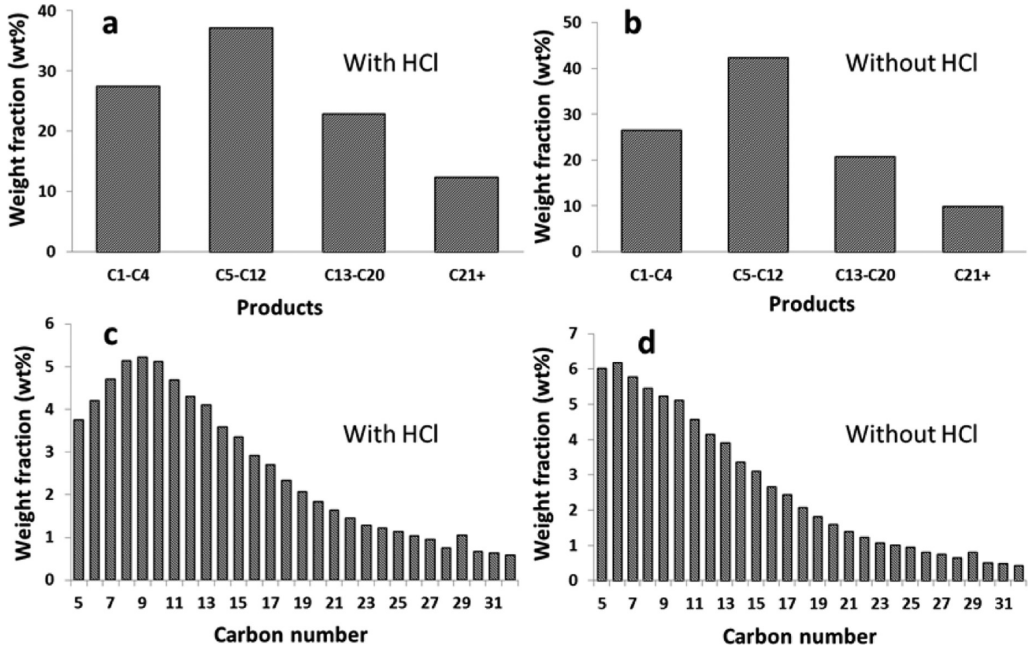

Figure 5. Weight distribution of hydrocarbon products obtained with and without HCl: (a and b) overall and (c and d) liquid phase.

dx.doi.org/10.1021/ef401198m | Energy Fuels 2013, 27, 6118−6124

another case, which may be taken as representative compounds of acid and N-containing tar impurities, respectively, both of which are known to poison FTS catalysts.[17] The amounts of HCl and pyridine added to the system corresponded to composition ranges of actual syngas from biomass gasification.[17] That is, for the HCl poison run, 5 mL of 0.012 M HCl in water was fed into the catalyst/10 mL of water/15 mL of decalin mixture in the reactor through a syringe after the reactor was cooled from the reduction step. Similarly, for the pyridine poison run, a mixture of 5 mL of water and 0.5 mL of pyridine was injected to the catalyst/water/decalin mixture. In each case, after loading the liquid mixture, the reactor was pressurized to 600 psi with syngas of $H_2/CO = 4$ and brought to the reaction temperature.

The results obtained in the HCl poison run are reported in Figure 5. The product distribution at CO conversion of 94.7% was very similar to that obtained without the addition of HCl. In contrast, the pyridine poison run did show some changes in conversion. However, it must be noted that the addition of pyridine to the decalin single-phase reaction results in a much lower conversion and a much broader spectrum of products than the run in the clean decalin single phase (see the Supporting Information for GC chromatographs).

The products include alkanes, alkene, long-chain alcohols, acids, and esters, clearly indicating the poisoning effect of pyridine. While conversion was also affected when the pyridine poison run was conducted in emulsion, the products only consisted of alkanes and alkylated piperidine, derived from pyridine. Moreover, they followed a uniform ASF-type distribution (see the Supporting Information). The partitions of pyridine, its hydrogenated product, piperidine, and alkylated piperidine products in water and organic phases are listed in Table 3. It can be seen that 86.3% of the pyridine and its

Table 3. Partition of Pyridine and Its Derivatives in Decalin and Water Phases after Reaction

partition (mol %)	decalin	water
pyridine	0.83	4.99
piperidine	3.73	81.35
alkylated piperidine	9.10	0
total in each phase	13.66	86.34

derivatives were captured in the water phase because of their high affinity to water. Certainly, one can see the potential benefits for elimination of these contaminants from the organic product.

Calculations of partitions of typical impurities in the water/oil phases were conducted assuming thermodynamic equilibrium under a range of temperatures and pressures common to FTS (150−250 °C and 600−1200 psi). Under these conditions, the calculated water/oil partitions indicate that H_2S is highly favored in the aqueous phase. In addition, calculated mass-transfer parameters for H_2S and NH_3 in water and decalin are shown in Table 4. While the two molecules have similar diffusion coefficients in both aqueous and organic phases, their mass-transport coefficients are smaller in the organic phase than in the aqueous phase. In addition, molar fluxes of H_2S and NH_3 are at least a factor of 2 smaller in the organic phase than in the aqueous phase. As a result, the undesired polar impurities would experience a higher transport resistance in the organic phase. Thus, the calculations lend support to the possibility of improving catalyst stability by

Table 4. Mass-Transfer Parameters of H_2S and NH_3 in Decalin and Water Phases

molecule	H_2S		NH_3	
phase	decalin	water	decalin	water
diffusion coefficient ($\times10^{-8}$, m^2/s)	3.42	3.94	3.91	4.51
mass-transport coefficient ($\times10^{-1}$, m/s)	0.942	1.12	1.06	1.26
concentration ($\times10^{-2}$, $kmol/m^3$)	1.31	2.98	3.09	5.96
molar flux ($\times10^{-3}$, kmol m^{-2} s^{-1})	1.23	3.33	3.28	7.52

adding additional resistance to transport of undesired polar impurities and, therefore, higher impurity tolerance in emulsion-phase FTS, as shown experimentally.

4. CONCLUSION

A novel multiphasic FTS system is proposed and demonstrated in this study, in which water and oil were mixed as the liquid reaction medium. The amphiphilic nature of the nanohybrid catalyst support used in the study facilitates the formation of the emulsion, in which the nanohybrid particles are stabilized at the water/oil interface. The FTS reaction conducted in the emulsion resulted in high CO conversion rates and a uniform ASF product distribution. Multiple potential benefits are envisioned for the FTS reaction in the emulsion system. One advantage of this system is that it allows for spontaneous product separation under reaction conditions purely based on solubility differences. This is especially significant for reactions like FTS that produce a wide range of products with different polarities and solubilities. In addition, a more restricted mass-transfer rate of impurities from the aqueous phase to the organic phase could greatly enhance impurity tolerance of FTS. One of the potential applications of the proposed system would be in FTS units with integrated syngas production by biomass gasification.

■ ASSOCIATED CONTENT

Ⓢ Supporting Information

Fitting product distribution with ASF equation, calculations of catalyst activity and TOF and water vapor during reduction and reaction steps, details and more results of calculations of partitions and mass transport of impurities, and GC chromatographs. This material is available free of charge via the Internet at http://pubs.acs.org.

■ AUTHOR INFORMATION

Corresponding Author

*E-mail: resasco@ou.edu.

Notes

The authors declare no competing financial interest.

■ ACKNOWLEDGMENTS

Financial support from the National Science Foundation (NSF)/Experimental Program to Stimulate Competitive Research (EPSCoR) Research Infrastructure Improvement Award (EPS 0814361) for the reaction part and from the U.S. Department of Energy (DOE)/EPSCoR (Grant DE SC0004600) for the emulsion and catalyst characterization part is gratefully acknowledged. We thank SouthWest Nanotechnologies, Inc. for the generous donation of CNTs.

■ REFERENCES

(1) Davis, B. H. *Catal. Today* **2002**, *71*, 249−300.

(2) Guettel, R.; Kunz, U.; Turek, T. *Chem. Eng. Technol.* **2008**, *31*, 746−754.
(3) Khadzhiev, S. N.; Lyadov, A. S.; Krylova, M. V.; Krylova, A. Y. *Pet. Chem.* **2011**, *51*, 24−31.
(4) Kölbel, H.; Ralek, M. *Catal. Rev.: Sci. Eng.* **1980**, *21*, 225−274.
(5) Van Steena, E.; Prinsloo, F. F. *Catal. Today* **2002**, *71*, 327−334.
(6) Garcia, J.; Gomes, H. T.; Serp, P.; Kalck, P.; Figueiredo, J. L.; Faria, J. L. *Catal. Today* **2005**, *102*, 101−109.
(7) Gomes, H. T.; Samant, P. V.; Serp, P.; Kalck, P.; Figueiredo, J. L.; Faria, J. L. *Appl. Catal., B* **2004**, *54*, 175−182.
(8) Yin, S.; Zhang, Q.; Xu, B.; Zhu, W.; Ng, C.; Au, C. *J. Catal.* **2004**, *224*, 384−396.
(9) Chen, H.; Lin, J.; Cai, Y.; Wang, X.; Yi, J.; Wang, J.; Wei, G.; Lin, Y.; Liao, D. *Appl. Surf. Sci.* **2001**, *180*, 328−335.
(10) Niesz, K.; Siska, A.; Vesselenyi, I.; Hernadi, K.; Mehn, D.; Galbacs, G.; Kónya, Z.; Kiricsi, I. *Catal. Today* **2002**, *76*, 3−10.
(11) Galvis, H. M. T.; Bitter, J. H.; Khare, C. B.; Ruitenbeek, M.; Dugulan, A.; de Jong, K. P. *Science* **2012**, *335*, 835−838.
(12) Kang, J.; Zhang, S.; Zhang, Q.; Wang, Y. *Angew. Chem., Int. Ed.* **2009**, *121*, 2603−2606.
(13) Crossley, S.; Faria, J.; Shen, M.; Resasco, D. E. *Science* **2010**, *327*, 68−72.
(14) Prada Silvy, R.; Tan, Y. Patent WO 2011/009071 A1, 2010.
(15) Shen, M.; Resasco, D. E. *Langmuir* **2009**, *25*, 10843−10851.
(16) Tomishige, K.; Asadullah, M.; Kunimori, K. *Catal. Today* **2004**, *89*, 389−403.
(17) Boerrigter, H.; Uil, H.; Calis, H. P. *Proceedings of the Pyrolysis and Gasification of Biomass and Waste Expert Meeting*; Strasbourg, France, Sept 30−Oct 1, 2002.
(18) Anderson, R. B. *Catalysts for the Fischer−Tropsch Synthesis*; Van Nostrand Reinhold: New York, 1956.
(19) Dry, M. E. *J. Mol. Catal.* **1982**, *17*, 133−144.
(20) Iglesia, E.; Reyes, S. C.; Madon, R. J. *J. Catal.* **1991**, *129*, 238−256.
(21) Schulz, H. *Appl. Catal., A* **1999**, *186*, 3−12.
(22) Wojciechowski, B. W. *Catal. Rev.: Sci. Eng.* **1988**, *30*, 629−702.
(23) Sarup, B.; Wojciechowski, B. W. *Can. J. Chem. Eng.* **1988**, *66*, 831−842.
(24) Kowalczyk, Z.; Stołecki, K.; Rarog-Pilecka, W.; Miskiewicz, E.; Wilczkowska, E.; Karpinski, Z. *Appl. Catal., A* **2008**, *342*, 35−39.
(25) Mieth, J. A.; Schwarz, J. A. *J. Catal.* **1989**, *118*, 203−217.
(26) Chen, Y.; Wang, H.; Goodwin, J. G.; Shiflett, W. K. *Appl. Catal.* **1983**, *8*, 303−314.
(27) Kellner, C. S.; Bell, A. T. *J. Catal.* **1982**, *75*, 251−261.
(28) Bezemer, G. L.; Bitter, J. H.; Kuipers, H. P. C. E.; Oosterbeek, H.; Holewijn, J. E.; Xu, X.; Kapteijn, F.; Van Dillen, A. J.; de Jong, K. P. *J. Am. Chem. Soc.* **2006**, *128*, 3956−3964.
(29) Claeys, M.; Van Steen, E. *Catal. Today* **2002**, *71*, 419−427.
(30) Storsæter, S.; Borg, Ø.; Blekkan, E. A.; Holmen, A. *J. Catal.* **2005**, *231*, 405−419.
(31) Krishnamoorthy, S.; Tu, M.; Ojeda, M. P.; Pinna, D.; Iglesia, E. *J. Catal.* **2002**, *211*, 422−433.
(32) Iglesia, E. *Appl. Catal., A* **1997**, *16* (1997), 59−78.
(33) Loveless, B.; Hibbitts, D.; Buda, C.; Lawlor, T.; Neurock, M.; Iglesia, E. *Proceedings of the 23rd North American Catalysis Society Meeting*; Louisville, KY, June 3−7, 2013.
(34) Madon, R. J.; Iglesia, E. *J. Mol. Catal.* **2000**, *163*, 189−204.
(35) Madon, R. J.; O'Connell, J. P.; Boudart, M. *AIChE J.* **1978**, *24*, 904−911.
(36) Forzatti, P.; Tronconi, E.; Pasquon, I. *Catal. Rev.: Sci. Eng.* **1991**, *33*, 109−168.
(37) Hancock, E. G. *Propylene and Its Industrial Derivatives*; Benn: London, U.K., 1973.
(38) De Klerk, A. *Fischer−Tropsch Refining*; Wiley-VCH: Weinheim, Germany, 2011.
(39) Iglesia, E.; Reyes, S. C.; Madon, R. J.; Soled, S. L. *Adv. Catal.* **1993**, *39*, 221−302.
(40) Smith, M. B.; March, J. *March's Advanced Organic Chemistry*, 5th ed.; Wiley: New York, 2001.
(41) Donnelly, T. J.; Satterfield, C. N. *Appl. Catal., A* **1989**, *52*, 93−114.
(42) Dictor, R. A.; Bell, A. T. *J. Catal.* **1986**, *97*, 121−136.
(43) Eliason, S. A.; Bartholomew, C. H. *Appl. Catal., A* **1999**, *186*, 229−243.
(44) Das, T. K.; Conner, W. A.; Li, J.; Jacobs, G.; Dry, M. E.; Davis, B. H. *Energy Fuels* **2005**, *19*, 1430−1439.
(45) Yates, I. C.; Satterfield, C. N. *Energy Fuels* **1991**, *5*, 168−173.
(46) Ojeda, M.; Nabar, R.; Nilekar, A. U.; Ishikawa, A.; Mavrikakis, M.; Iglesia, E. *J. Catal.* **2010**, *272*, 287−297.
(47) Bain, R. L.; Dayton, D. C.; Carpenter, D. L.; Czernik, S. R.; Feik, C. J.; French, R. J.; Magrini-Bair, K. A.; Phillips, S. D. *Ind. Eng. Chem. Res.* **2005**, *44*, 7945.